Regulatory Role of *SGT1* in Early *R* Gene–Mediated Plant Defenses

Mark J. Austin,[1] Paul Muskett,[1] Katherine Kahn,[1] Bart J. Feys,[1] Jonathan D. G. Jones,[1] Jane E. Parker[1,2]*

Animal SGT1 is a component of Skp1-Cullin–F-box protein (SCF) ubiquitin ligases that target regulatory proteins for degradation. Mutations in one (*SGT1b*) of two highly homologous *Arabidopsis SGT1* genes disable early plant defenses conferred by multiple resistance (*R*) genes. Loss of *SGT1b* function in resistance is not compensated for by *SGT1a*. *R* genes differ in their requirements for *SGT1b* and a second resistance signaling gene, *RAR1*, that was previously implicated as an SGT1 interactor. Moreover, *SGT1b* and *RAR1* contribute additively to *RPP5*-mediated pathogen recognition. These data imply both operationally distinct and cooperative functions of SGT1 and RAR1 in plant disease resistance.

In plants, a major form of resistance to disease caused by microbial pathogens is by expression of complementary gene pairs in the plant and pathogen, known respectively as resistance (*R*) and avirulence (*avr*) genes (*1*). Direct or indirect interaction of their products activates cellular defenses that prevent pathogen colonization of the plant. Failure to express either component results in disease susceptibility. The predominant class of *R* gene in a diverse range of species encodes cytoplasmic proteins that resemble Nod proteins involved in animal innate immunity (*1, 2*). Plant Nod-like proteins possess a central nucleotide-binding (NB)/apoptotic adenosine triphosphatase–homologous domain, COOH-terminal leucine-rich repeats (LRRs), and NH_2-terminal portions that either resemble the cytoplasmic domains of *Drosophila* and human Toll-like receptors [Toll–interleukin-1–resistance (TIR) domains] or contain a coiled-coil (CC) motif. Resistance conditioned by NB-LRR proteins is commonly associated with rapid, localized programmed cell death known as the hypersensitive response (HR) and an oxidative burst producing reactive oxygen intermediates (ROI) (*3*).

The *RPP5* gene in *Arabidopsis* accession Landsberg *erecta* (Ler) encodes a TIR–NB-LRR protein conferring resistance to the downy mildew pathogen *Peronospora parasitica* (*4*). We undertook mutational screens to identify other essential genes in *RPP5* resistance and have identified multiple, independent recessive mutations at four loci (*5*). Two of these, *EDS1* and *PAD4*, encode lipase-like proteins that are engaged by TIR–NB-LRR type proteins but are dispensible in resistance conditioned by CC–NB-LRR proteins (*6–9*). The third gene is the single *Arabidopsis* ortholog of barley *RAR1* (*10*), a necessary component of *R* gene–mediated resistance to the powdery mildew fungus (*11*). *RAR1* encodes a 25-kD cytoplasmic protein with two zinc-binding CHORDs (cysteine-

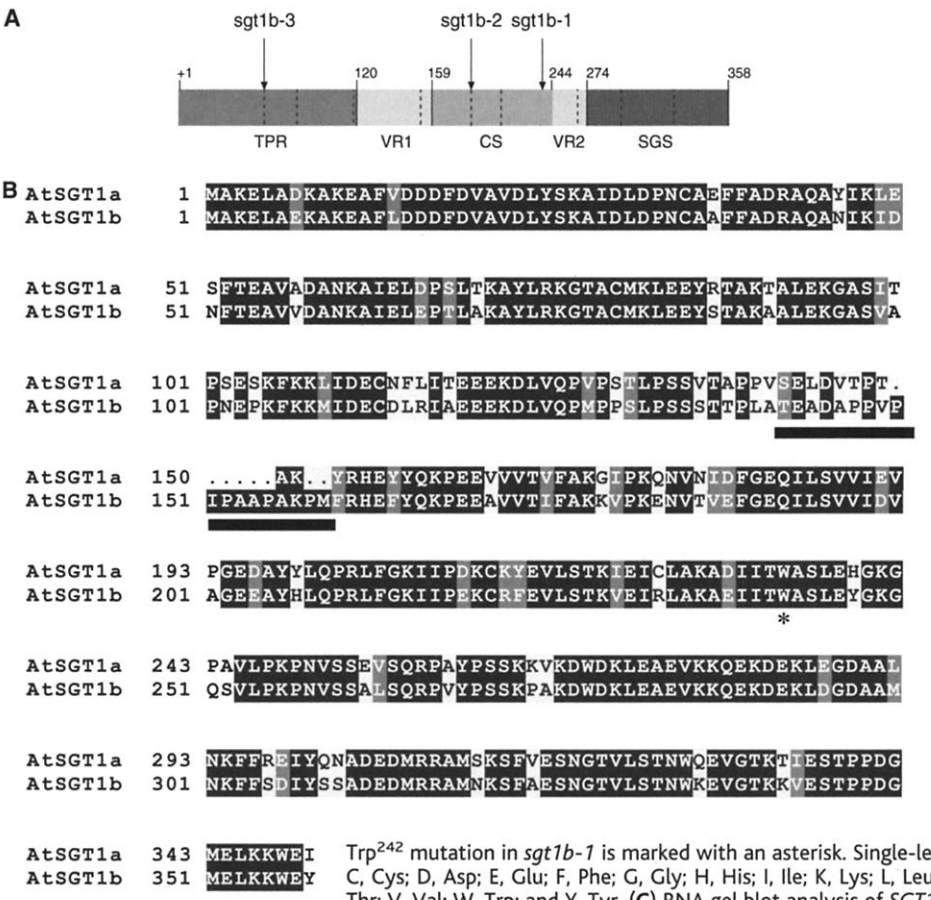

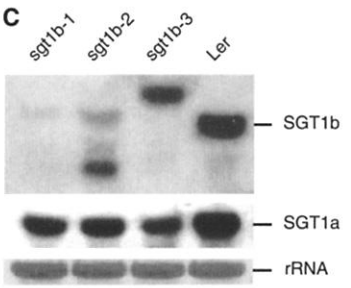

Fig. 1. Sequence analysis of *Arabidopsis SGT1a* and *SGT1b*. (**A**) Plant SGT1 has been assigned several domains (*12, 15*): TPR, tetratricopeptide repeats; CS, CHORD protein and SGT1–specific; SGS, SGT1-specific motif; VR1 and VR2, variable domains. Three independent mutations were identified in *Arabidopsis SGT1b*. In *sgt1b-1*, a nucleotide substitution changes $Trp^{242} \rightarrow$ stop, causing a predicted protein truncation. *sgt1b-2* is mutated within the intron 5 consensus splice acceptor site (G1317 → A). *sgt1b-3* has a single-nucleotide mutation within the intron 1 splice donor site (G161 → A). (**B**) Sequence alignment between *Arabidopsis* SGT1a and SGT1b shows 78.3% amino acid identity. SGT1a and SGT1b are, respectively, 28.8% and 27.3% identical to yeast SGT1. Black and shaded boxes indicate identical and >50% conserved residues, respectively. A black line below SGT1b amino acids 140 to 159 shows the peptide sequence used to derive SGT1b-specific antisera. The Trp^{242} mutation in *sgt1b-1* is marked with an asterisk. Single-letter abbreviations for amino acid residues: A, Ala; C, Cys; D, Asp; E, Glu; F, Phe; G, Gly; H, His; I, Ile; K, Lys; L, Leu; M, Met; N, Asn; P, Pro; Q, Gln; R, Arg; S, Ser; T, Thr; V, Val; W, Trp; and Y, Tyr. (**C**) RNA gel blot analysis of *SGT1a* and *SGT1b* transcripts in mutant and wild-type plants. Total RNA from wild-type (Ler) and *sgt1b* mutant lines was probed with *SGT1a*- or *SGT1b*-specific radiolabeled cDNAs.

and histidine-rich domains) that are conserved in sequence and tandem organization among all eukaryotic phyla examined (*12*). Metazoan CHORD proteins possess a motif (the CS domain) that is exclusively shared with SGT1 (*12*), an essential component of cell cycle progression via SKP1-mediated activation of the kinetochore complex CBF3 in yeast (*13*). Yeast SGT1 also associates with the SCF ubiquitin ligase complex by interaction with SKP1 and is required for SCF-mediated protein ubiquitylation in vitro (*13*).

We identified the fourth locus essential for *Arabidopsis RPP5* resistance as one (*SGT1b*) of two *SGT1* homologs (*14*). Although the predicted *Arabidopsis* SGT1a and SGT1b proteins are highly sequence related, only mutations in *SGT1b* were isolated in screens for components of *RPP5* resistance (Fig. 1, A and B). The conserved intron/exon structures of *SGT1a* and *SGT1b* (*14*), coupled with higher sequence relatedness between them than with other plant *SGT1* homologs (*15*), suggest that they have arisen by recent gene duplication (*16*). A combination of RNA gel blot (Fig. 1C) and RNA quantification using Taqman chemistry (*5*) revealed defects in *SGT1b* but not *SGT1a* transcripts in the *sgt1b* mutants. Thus, *SGT1b* is a necessary and nonredundant component of *RPP5*-mediated resistance.

We examined the relative levels of SGT1a and SGT1b proteins in soluble extracts from wild-type and *sgt1b* mutant plants (*5*). Probing protein blots with antibodies raised against the conserved SGS domain of SGT1 (*15*) showed that SGT1b was undetectable in all three *sgt1b* lines (Fig. 2A). SGT1a was not depleted in the *sgt1b* mutants, indicating unaltered stability of SGT1a in the absence of SGT1b (Fig. 2A). SGT1b was not detectable in *sgt1b-1*, *sgt1b-2*, and *sgt1b-3* extracts probed with an SGT1b-specific antibody; hence, all of them may be null mutations (Fig. 2B). This conclusion is consistent with the observation that each *sgt1b* allele exhibited an equivalent loss of *RPP5* resistance. We reasoned that the *sgt1b* phenotype is likely to be due to defects specifically in *SGT1b*.

Levels of SGT1b were unaffected by mutations in each of the *RPP5* resistance signaling components *RAR1*, *EDS1*, and *PAD4* (Fig. 2B). SGT1b expression also did not change after inoculation of wild-type leaves with pathogen isolate *P. parasitica* Noco2 that is recognized by *RPP5* (Fig. 2C). Similar results were obtained in tissues of *rpp5* mutant plants that fail to recognize Noco2 and therefore allow pathogen colonization (Fig. 2C). PR1, a marker of downstream plant defenses, was induced in inoculated wild-type (*RPP5*) but not in control samples (Fig. 2D), indicating that resistance was appropriately elicited in these experiments. Therefore, pathogen infection does not alter SGT1b expression substantially, although we cannot rule out that changes in SGT1b abundance occur transiently or in a restricted number of cells at pathogen penetration sites.

We compared the defects of *sgt1b-1* with other mutant lines that compromise *RPP5* by measuring the extent of pathogen asexual sporulation and plant cell necrosis on infected leaves. Loss of *RPP5* resistance in *sgt1b* was equivalent to that in a *rar1* null mutant but was not as strong as in null *rpp5* or *eds1* plants that exhibited, respectively, susceptibility and supersusceptibility (Fig. 3A) (*4, 9*). A double *sgt1b/rar1* mutant exhibited additive disease susceptibility equivalent to *rpp5* (Fig. 3A), indicating that wild-type *SGT1b* and *RAR1* operate genetically independently of each other in *RPP5* resistance. Examination of inoculated leaves under ultraviolet light revealed occasional plant cell death–associated autofluorescence in *sgt1b* and *rar1* but not in *rpp5*, *eds1*, or *sgt1b/rar1* (Fig. 3B). By microscopic analysis, we estimated that the HR was disabled in ~95% of pathogen inoculation sites of *sgt1b* (Fig. 3C) and *rar1* (*10*), contrasting with a complete suppression

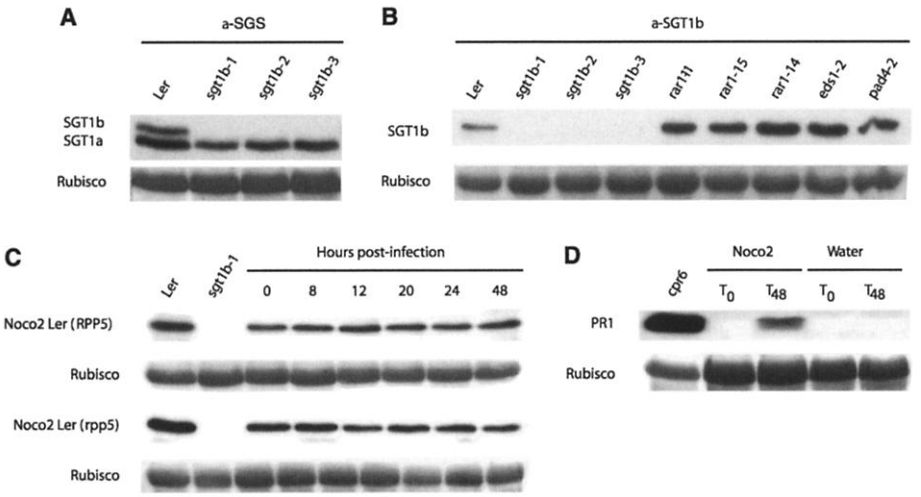

Fig. 2. Analysis of SGT1a and SGT1b protein expression. Immunoblots of total protein extracts from wild-type Ler, *sgt1b* mutants, partial (*rar1-14*, *rar1-15*) and null (*rar1-11*) *rar1* (*10*), *eds1-2* (*9*), and *pad4-2* (*8*) mutant lines were probed with antibody to SGS (a-SGS) (**A**) that detects SGT1a and SGT1b (*15*) or with an antibody specific for SGT1b (a-SGT1b) (**B**) (*5*). (**C**) Blots of total protein extracted from Ler (*RPP5*) or Ler (*rpp5*) (*4*) plants after inoculation with *P. parasitica* isolate Noco2 were probed with antibody to SGT1b. (**D**) Expression of the defense marker PR1 in Noco2-inoculated or water-treated Ler (*RPP5*) plants was measured using *Arabidopsis* antibody to PR1 (*24*). Extract from *cpr6*, which constitutively expresses *PR* genes (*25*), was used as a positive control. T_0 and T_{48} indicate time elapsed since treatment. In all panels, Rubisco (ribulose-1,5-bisphosphate carboxylase-oxygenase) was used as a protein loading control.

Table 1. Different *Arabidopsis R* gene requirements for *SGT1b* and *RAR1*. Disease resistance (R), susceptibility (S), or partial susceptibility [(S)] was scored on the basis of asexual sporulation levels of *P. parasitica* isolates or bacterial growth of *P. syringae* strains (*5*). All *R* genes tested were expressed in the Ler background except *RPP2* and *RPP4* in accession Columbia and *RPP1A* in Wassileskija that were individually combined with *sgt1b-1* or *rar1-10* in segregating F_2 populations (*5, 10*). TIR and CC domains of cloned NB-LRR genes are indicated (*5*).

Pathogen	Isolate/strain	*R* gene	NB-LRR protein	Mutant phenotype	
				sgt1b	*rar1*
Peronospora parasitica	Noco2	*RPP5*	TIR	S	S
	Cala2	*RPP2*	TIR	S	R
	Emwa1	*RPP4*	TIR	S	S
	Cala2	*RPP1A*	TIR	R	R
	Emco5	*RPP8*	CC	R	R
	Maks9	*RPP21*	?	(S)	(S)
P. s. pv. *tomato* DC3000	*avrRps4*	*RPS4*	TIR	R	S
	avrRpt2	*RPS2*	CC	R	S
	avrRpm1	*RPM1*	CC	R	S

[1]Sainsbury Laboratory, John Innes Centre, Colney Lane, Norwich NR4 7UH, UK. [2]Max Planck Institute for Plant Breeding Research, Carl-von-Linné Weg 10, D-50829 Cologne, Germany.

*To whom correspondence should be addressed. E-mail: parker@mpiz-koeln.mpg.de

of HR in *rpp5* (Fig. 3C). Substantially delayed plant cell death in *sgt1b* was evident later in infection by appearance of necrotic plant cells trailing the pathogen (Fig. 3C). Whole-cell ROI accumulation was undetectable at most pathogen inoculation sites of *sgt1b* and *rar1* but was occasionally observed in cells at later stages of colonization (*17*). These data reveal cooperation between SGT1 and RAR1 in the regulation of *RPP5*-triggered cell death and the oxidative burst.

In *Arabidopsis*, *RAR1* is essential for resistance conferred by multiple *R* genes recognizing distinct avirulent *P. parasitica* or *Pseudomonas syringae* pv. *tomato* isolates (*10*). We found that these *R* genes have either common or separate genetic requirements for *RAR1* and *SGT1b* (Fig. 3D and Table 1). These findings provide evidence that SGT1b and RAR1 have overlapping but nonidentical roles in resistance triggered by different *R* genes. Usage of *RAR1* and/or *SGT1b* was not restricted to a particular NB-LRR structural type (Table 1), whereas *EDS1* and *PAD4* are specifically required by TIR–NB-LRR proteins (*6, 9*).

In yeast, the cellular roles of SGT1 are closely linked to its association with SKP1, an integral ubiquitin ligase protein (*13*). A mouse homolog of SGT1 was also identified by mass spectrometry as an SCF interactor (*18*). The sequence relatedness of *Arabidopsis* SGT1a and SGT1b (Fig. 1B), coupled with the ability of both genes to complement two yeast temperature-sensitive *sgt1* mutant alleles (*15*), suggests that fundamental cellular function(s) of yeast *SGT1* in SCF-mediated protein ubiquitylation (*13, 19, 20*) are retained by both *Arabidopsis SGT1* ho-

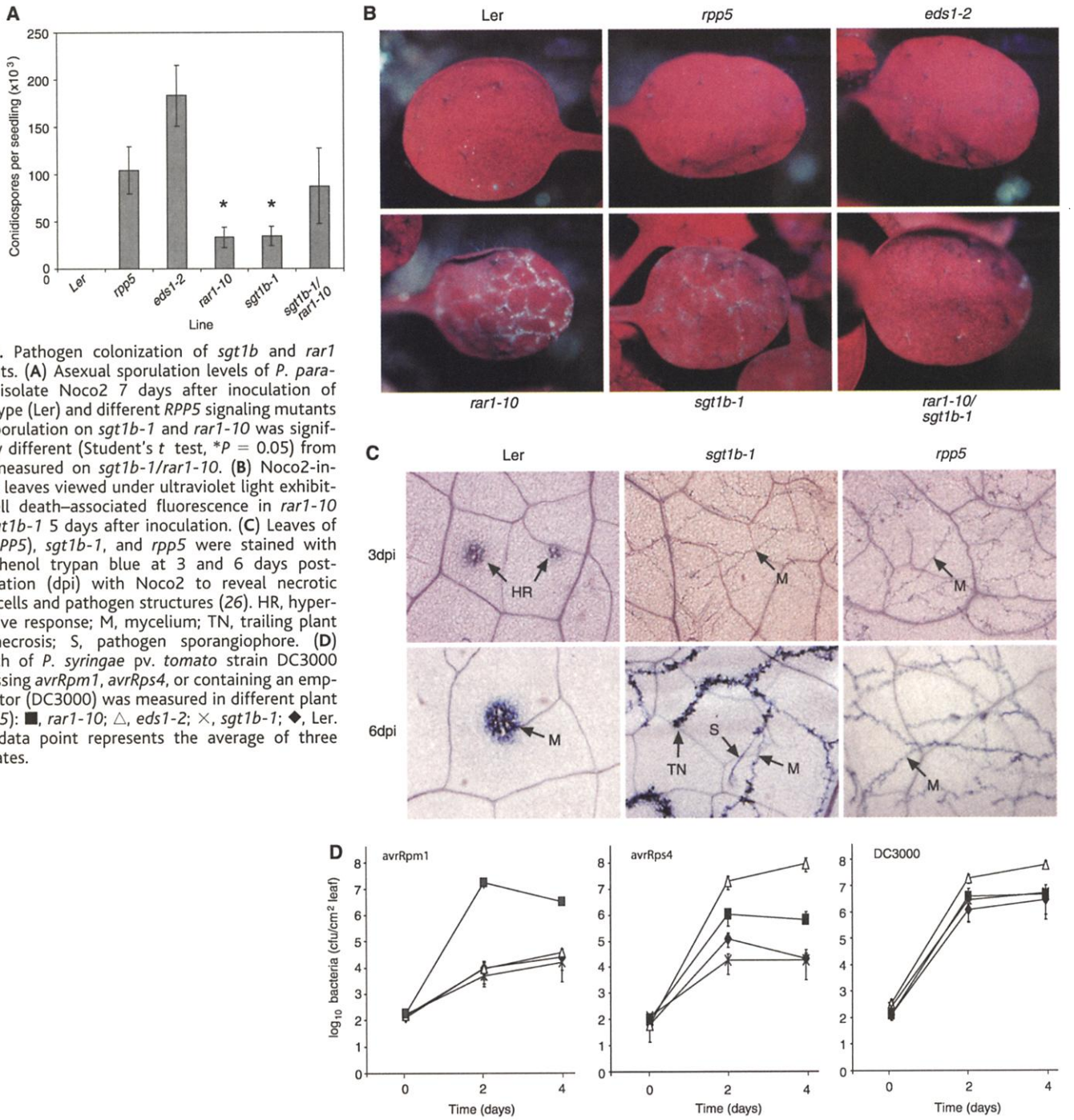

Fig. 3. Pathogen colonization of *sgt1b* and *rar1* mutants. (**A**) Asexual sporulation levels of *P. parasitica* isolate Noco2 7 days after inoculation of wild-type (Ler) and different *RPP5* signaling mutants (*5*). Sporulation on *sgt1b-1* and *rar1-10* was significantly different (Student's *t* test, $^*P = 0.05$) from that measured on *sgt1b-1/rar1-10*. (**B**) Noco2-infected leaves viewed under ultraviolet light exhibiting cell death–associated fluorescence in *rar1-10* and *sgt1b-1* 5 days after inoculation. (**C**) Leaves of Ler (*RPP5*), *sgt1b-1*, and *rpp5* were stained with lactophenol trypan blue at 3 and 6 days post-inoculation (dpi) with Noco2 to reveal necrotic plant cells and pathogen structures (*26*). HR, hypersensitive response; M, mycelium; TN, trailing plant cell necrosis; S, pathogen sporangiophore. (**D**) Growth of *P. syringae* pv. *tomato* strain DC3000 expressing *avrRpm1*, *avrRps4*, or containing an empty vector (DC3000) was measured in different plant lines (*5*): ■, *rar1-10*; △, *eds1-2*; ×, *sgt1b-1*; ◆, Ler. Each data point represents the average of three replicates.

mologs. We present evidence that *SGT1b* has evolved a distinct capability in certain *R* gene–specified responses that is not compensated for by *SGT1a*. Nonredundant functions of *Arabidopsis* SGT1a and SGT1b in plant defense may reflect preferential interactions with different subsets of SCF complexes. Representation of at least 19 *SKP1* orthologs and >300 F-box–containing proteins in the *Arabidopsis* genome creates the potential for considerable flexibility in SCF composition and regulatory function (*16, 21–23*).

Our data show that *RAR1* and *SGT1b* each contribute quantitatively to *RPP5*-dependent resistance and are thus operationally distinct. It is noteworthy that Azevedo *et al.* (*15*) show conserved molecular association between plant SGT1 and RAR1, including *Arabidopsis* SGT1a and SGT1b. In barley extracts, SGT1 exists in two pools, one containing RAR1, the other engaging SCF components. The combined genetic and molecular data imply that SGT1-RAR1 and SGT1-SCF complexes have at least partially distinct roles in disease resistance. In one scenario, mutations in *RAR1* but not *SGT1a* or *SGT1b* might disable SGT1-RAR1 function, whereas mutations in *SGT1b* might compromise a subset of SCF complexes that are preferentially used in *R* gene–triggered responses. Such a model would account for the exclusive genetic requirements of certain *R* genes for either *RAR1* or *SGT1b*, directing signals through one or the other mechanism to trigger plant defense.

References and Notes

1. J. L. Dangl, J. D. G. Jones, *Nature* **411**, 826 (2001).
2. N. Inohara *et al.*, *J. Biol. Chem.* **275**, 27823 (2000).
3. J. Cohn, G. Sessa, G. B. Martin, *Curr. Opin. Immunol.* **13**, 55 (2001).
4. J. E. Parker *et al.*, *Plant Cell* **9**, 879 (1997).
5. See supplemental material on *Science* Online at www.sciencemag.org/cgi/content/full/1067747/DC1.
6. N. Aarts *et al.*, *Proc. Natl. Acad. Sci. U.S.A.* **95**, 10306 (1998).
7. A. Falk *et al.*, *Proc. Natl. Acad. Sci. U.S.A.* **96**, 3292 (1999).
8. D. Jirage *et al.*, *Proc. Natl. Acad. Sci. U.S.A.* **96**, 13583 (1999).
9. B. J. Feys, L. J. Moisan, M. A. Newman, J. E. Parker, *EMBO J.* **20**, 5400 (2001).
10. P. Muskett *et al.*, *Plant Cell*, in press.
11. J. H. Jørgensen, *Genome* **39**, 492 (1996).
12. K. Shirasu *et al.*, *Cell* **99**, 355 (1999).
13. K. Kitegawa *et al.*, *Mol. Cell* **4**, 21 (1999).
14. A positional cloning strategy was used to map three allelic, recessive mutations in *Arabidopsis* accession Landsberg *erecta* (Ler) to a 50-kb interval on the lower arm of chromosome 4 [bacterial artificial chromosome (BAC) F8L21] [Munich Information Center for Protein Sequences (MIPS) *Arabidopsis thaliana* Group, www.mips.biochem.mpg.de/proj/thal]. Direct DNA sequencing of candidate genes within this region identified mutations in a gene with homology to yeast *SGT1*, denoted *SGT1b* (GenBank accession number AF439976). There are two *SGT1* homologs in genomic DNA of *Arabidopsis* accession Columbia (Col-0) (www.mips.biochem.mpg.de/proj/thal). *SGT1a* (BAC F9D16; GenBank accession number AF439975) is linked by 6 Mb to *SGT1b* on chromosome 4. Ler *SGT1a* and *SGT1b* intron/exon structures were verified by sequencing genomic DNA. Ler and Col-0 SGT1b proteins are identical. Ler and Col-0 SGT1a differ by a single amino acid (residue 224). The presence of two Ler *SGT1* genes was confirmed on genomic DNA gel blots.
15. C. Azevedo *et al.*, *Science* **295**, 2073 (2002); published online 14 February 2002 (10.1126/science.1067554).
16. The *Arabidopsis* Genome Initiative, *Nature* **408**, 796 (2000).
17. M. J. Austin *et al.*, data not shown.
18. S. Lyapina *et al.*, *Science* **292**, 1382 (2001).
19. R. J. Deshaies, *Annu. Rev. Cell Dev. Biol.* **15**, 435 (1999).
20. J. Callis, R. D. Vierstra, *Curr. Opin. Plant Biol.* **3**, 381 (2000).
21. M. A. Andrade, M. González-Guzmán, R. Serrano, P. L. Rodríguez, *Plant Mol. Biol.* **46**, 603 (2001).
22. R. Ferrás *et al.*, *EMBO J.* **20**, 2742 (2001).
23. W. M. Gray, S. Kepinski, D. Rouse, O. Leyser, M. Estelle, *Nature* **414**, 271 (2001).
24. D. J. Kliebenstein *et al.*, *Mol. Plant-Microbe Interact.* **12**, 1022 (1999).
25. J. D. Clarke, Y. Liu, D. F. Klessig, X. Dong, *Plant Cell* **10**, 557 (1998).
26. E. Koch, A. Slusarenko, *Plant Cell* **2**, 437 (1990).

27. Supported by the Gatsby Charitable Foundation, a BBSRC grant (J.P.), and an EMBO long-term fellowship (K.K.). We thank R. Last (Boyce Thompson Institute for Plant Research, Cornell University, Ithaca, NY) for antibody to PR1, and A. Sadanandom and K. Shirasu (Sainsbury Laboratory, Norwich, UK) for antibody to SGS.

5 November 2001; accepted 17 January 2002
Published online 14 February 2002;
10.1126/science.1067747
Include this information when citing this paper.

Structure of HP1 Chromodomain Bound to a Lysine 9–Methylated Histone H3 Tail

Steven A. Jacobs and Sepideh Khorasanizadeh*

The chromodomain of the HP1 family of proteins recognizes histone tails with specifically methylated lysines. Here, we present structural, energetic, and mutational analyses of the complex between the *Drosophila* HP1 chromodomain and the histone H3 tail with a methyllysine at residue 9, a modification associated with epigenetic silencing. The histone tail inserts as a β strand, completing the β-sandwich architecture of the chromodomain. The methylammonium group is caged by three aromatic side chains, whereas adjacent residues form discerning contacts with one face of the chromodomain. Comparison of dimethyl- and trimethyllysine-containing complexes suggests a role for cation-π and van der Waals interactions, with trimethylation slightly improving the binding affinity.

Although the structure of the nucleosome core particle is known, the histone tails, which protrude from the nucleosome core and undergo posttranslational modifications, have not been observed (*1*, *2*). A "histone code" hypothesis suggests that covalent modification of these tails, such as acetylation, phosphorylation, and methylation, creates a favorable docking surface for protein modules that interact with chromatin in a manner that may extend the genetic code (*3*). The sites of lysine methylation on histone tails have been known for 30 years, but direct evidence linking them to gene activity has only appeared recently. On histone H3, methylation at Lys^9 (MeK9 H3) produces a site for HP1 (heterochromatin-associated protein 1) binding, and is associated with epigenetic silencing in organisms as diverse as fission yeast and mammals (*4–8*). We recently showed that the chromodomain of *Drosophila* HP1 is sufficient for specific interactions with the histone H3 tail, in a manner that depends on the methylation of Lys^9 (*7*). Here, we show the structural and energetic determinants of this interaction to further elucidate the mechanism of methyllysine recognition, as well as histone H3 tail recognition by the chromodomain.

We used a pair of synthetic peptides corresponding to residues 1 to 15 of histone H3, which included dimethyllysine (Me_2K) and also trimethyllysine (Me_3K) at residue 9 (*9*). We used isothermal titration calorimetry to measure the affinity of the HP1 chromodomain for both Me_2K- and Me_3K-bearing peptides, and found these to be 7 and 2.5 μM, respectively (*9*). To visualize the chromodomain interaction with the H3 tail, we formed its complexes with these peptides and obtained crystals for x-ray diffraction studies. The structures were solved at 2.1 and 2.4 Å resolutions, respectively (*9*). Analysis of the $|2F_o - F_c|$ and $|F_o - F_c|$ difference maps clearly indicated electron density for the bound position of the H3 peptide in both complexes (Fig. 1A). We did not see residues 1 to 4 or 11 to 15 of the peptides, suggesting that only residues Gln^5-

Department of Biochemistry and Molecular Genetics, University of Virginia Health System, Charlottesville, VA 22908–0733, USA.

*To whom correspondence should be addressed. E-mail: khorasan@virginia.edu